

# A general heavy-flavor mass scheme for charged-current DIS at NNLO and beyond

Jun Gao<sup>1,2</sup>, T. J. Hobbs<sup>3,4,5</sup>, P. M. Nadolsky<sup>3</sup>, ChuanLe Sun<sup>1,2</sup>, C.-P. Yuan<sup>6</sup>

<sup>1</sup> *INPAC, Shanghai Key Laboratory for Particle Physics and Cosmology*

*& School of Physics and Astronomy, Shanghai Jiao Tong University, Shanghai 200240, China*

<sup>2</sup> *Key Laboratory for Particle Astrophysics and Cosmology (MOE), Shanghai 200240, China*

<sup>3</sup> *Department of Physics, Southern Methodist University, Dallas, TX 75275-0175, USA*

<sup>4</sup> *Department of Physics, Illinois Institute of Technology, Chicago, IL 60616, USA*

<sup>5</sup> *Jefferson Lab, EIC Center, Newport News, VA 23606, USA*

<sup>6</sup> *Department of Physics and Astronomy, Michigan State University, East Lansing, MI 48824, USA*

(Dated: July 2, 2021)

We present a computation for inclusive charged-current deeply-inelastic scattering at NNLO (N<sup>2</sup>LO) in QCD. Mass-dependent quark contributions are consistently included across a wide range of momentum transfers in the SACOT- $\chi$  general-mass scheme. When appropriate, we further include N<sup>3</sup>LO corrections in the zero-mass scheme. We show theoretical predictions for several experiments with neutrinos over a wide range of energies and at the upcoming Electron-Ion Collider. Our prediction reduces perturbative uncertainties to  $\sim 1\%$ , sufficient for the high-precision objectives of future charged-current DIS measurements.

Charged-current deeply-inelastic scattering (CC DIS) has the potential to unlock unique combinations of quark-flavor currents inside QCD matter and is therefore a useful complement to neutral-current (NC) DIS as a probe of hadronic and nuclear structure. There have been numerous CC DIS measurements from fixed-target experiments (see Ref. [1] for an overview) as well as from HERA [2]. In addition, as a dominant contribution to the total inclusive CC cross section for (anti)neutrino scattering off nuclei at  $E_\nu \sim [\text{few GeV}]$  and beyond, CC DIS plays an essential role in various neutrino experiments, including the upcoming Deep Underground Neutrino Experiment (DUNE) at Fermilab [3], the IceCube neutrino telescope [4], and FASER $\nu$  [5] at the LHC. An enhanced theoretical understanding of the neutrino DIS cross section will therefore advance the precision objectives of several neutrino experiments operating over a wide energy spectrum. Such theoretical improvements will also be relevant for the future Electron-Ion Collider (EIC) [6–8], which, like HERA, will exploit CC DIS to explore the flavor dependence of hadrons’ three-dimensional structure.

Control over heavy-quark (HQ) contributions is vital to achieving high-precision in theoretical calculations of DIS cross sections. Implementation of HQ contributions depends on the treatment of quark masses in conjunction with the organization of the perturbative expansion [9–11]. Wilson coefficients with massive quark lines must be calculated within the same factorization scheme as the one adopted to evaluate running of the strong coupling  $\alpha_s$  and to extract parton distributions functions (PDFs) from a global analysis of experimental data. For example, the CT18 PDFs [12] were extracted in the Simplified-ACOT- $\chi$  (SACOT- $\chi$ ) scheme [13–17]. Hence, when using CT PDFs in a theory calculation, the needed Wilson coefficients should also be consistently calculated in that scheme, as required by the factorization theorem.

In the Wilson coefficients for high-energy processes, a

HQ mass  $M_Q$  can be set to zero when it is substantially smaller than the typical momentum scale  $Q$ . Within this *massless* approximation, the heavy quark actively participates in the running of  $\alpha_s$  and evolution of PDFs. On the other hand, when  $Q$  is comparable to  $M_Q$ , the relevant Wilson coefficients must include the heavy-quark mass dependence. At such  $Q$ , it is economical to use a *fixed-flavor number* (FFN) factorization scheme in which neither  $\alpha_s$  nor the PDFs receive contributions from the massive quark flavor.

General-mass (GM) factorization schemes are comprehensive frameworks to predict the full heavy-mass dependence and have been widely used in modern PDF global analyses. These schemes have been deployed in a variety of contexts, including DIS [16–20] and  $pp$  hadroproduction [21–25]. General-mass variable flavor number (GM-VFN) schemes interpolate between the two extremes noted above, in which a GM calculation involving  $N_f + 1$  parton flavors matches onto a FFN scheme with  $N_f$  flavors at  $Q \sim M_Q$  while converging to a zero-mass (ZM) scheme at  $Q \gg M_Q$ , thereby fully specifying the relevant cross section over a broad range of  $Q$ .

In this Letter we employ the SACOT- $\chi$  GM scheme to present the first calculation of inclusive CC DIS at next-to-next-to-leading order (N<sup>2</sup>LO) in QCD with full mass dependence. Derived from the all-orders proof of QCD factorization for DIS with massive quarks [15], the SACOT- $\chi$  scheme offers crucial advantages: simpler implementation of mass dependence, stable perturbative convergence, and control of partonic threshold effects. The  $\chi$ -rescaling prescription [17] streamlines the matching onto the FFN prediction near the threshold. This is achieved by using mass-dependent phase space for all HQ contributions, which works both in DIS and hadroproduction [26]. We will outline the SACOT- $\chi$  theoretical framework for CC DIS and apply it to several phenomenological studies.

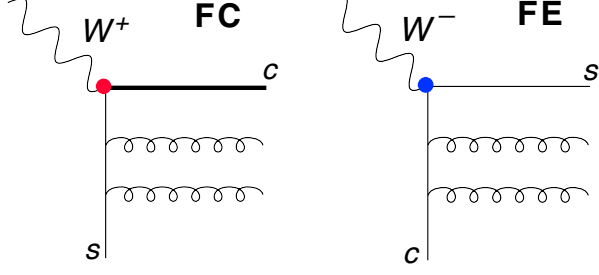


FIG. 1: Representative CC DIS diagrams at N<sup>2</sup>LO for either flavor creation (left) or excitation (right), with the latter being effectively proportional to the HQ PDF.

### THE SACOT- $\chi$ SCHEME

We proceed by extending the previous realization of the SACOT- $\chi$  scheme in Ref. [27] for neutral-current DIS at N<sup>2</sup>LO to the analogous problem in the charge-current sector, explicitly tracing the HQ mass dependence through various radiative contributions at  $\mathcal{O}(\alpha_s^2)$ . We first demonstrate this method on the DIS structure functions,  $F = F_1, F_2, F_3$ , before computing DIS reduced cross sections. Up to N<sup>2</sup>LO, QCD factorization allows a structure function to be written as a convolution of parton-level coefficient functions,  $C_{i,j}$ , and nonperturbative correlation functions,  $\Phi$ , *i.e.*, the PDFs, as,

$$F(x, Q) = \sum_i \sum_j \{C_{i,j} \otimes \Phi_j\}(x, Q) \equiv F_l(x, Q) + F_h(x, Q), \quad (1)$$

where “ $\otimes$ ” denotes a convolution over the momentum fraction  $z$ , and we do not show the electroweak couplings, including the CKM matrix elements, for simplicity. The equation sums over contributions from relevant active parton flavors ( $j$ ) in the initial state and parton flavors ( $i$ ) produced in the final state. In order to implement the proper HQ mass dependence, it is necessary to decompose the convolution in the RHS of Eq. (1) according to the topology and flavor structure of the participating Feynman diagrams. In this work, we take the maximum number of active quark flavors inside the nucleon to be  $N_f = 4$ , together with the gluon.

Each structure function  $F(x, Q)$  is a sum of  $F_l(x, Q)$  and  $F_h(x, Q)$  defined as follows:

- $F_l$  contains contributions in which only light-quark flavors ( $q_l$ ) are directly coupled to the  $W^\pm$  boson via the  $Wq_l\bar{q}_l$  vertex.
- $F_h$  contains contributions involving  $Wq_h\bar{q}_l$  or  $Wq_l\bar{q}_h$  vertices. Here,  $q_l$  denotes the  $u, d$  and  $s$  quarks, and  $q_h$  the charm quark.

Contributions to  $F_l$  and  $F_h$  can be classified as representing either *flavor excitation* (FE) or *flavor creation* (FC) depending on whether the heavy quark appears in the initial state or only the final and virtual states. In CC DIS,  $F_l$  receives HQ contributions starting from N<sup>2</sup>LO, while there are both FE and FC diagrams for  $F_h$  at LO. Two representative Feynman diagrams for  $F_h$  at N<sup>2</sup>LO are shown in Fig. 1. The Wilson coefficients  $C_{i,j}(z)$  can be expanded in the QCD coupling  $a_s \equiv \alpha_s(\mu, N_f)/(4\pi)$  as

$$C_{i,j}(z) = C_{i,j}^{(0)} + a_s C_{i,j}^{(1)} + a_s^2 C_{i,j}^{(2)} + \mathcal{O}(a_s^3), \quad (2)$$

with the LO coefficients given by

$$C_{l,l}^{(0)} = \delta(1-z), \quad C_{h,h}^{(0)} = \delta(1-\chi), \\ C_{h,l}^{(0)} = \delta(1-\chi), \quad \chi \equiv (1 + m_c^2/Q^2)z, \quad (3)$$

where  $C_{h,l}^{(0)}$  and  $C_{h,h}^{(0)}$  correspond to FC and FE contributions, respectively. At NLO, there are gluon contributions to  $F_l$  and  $F_h$ ,

$$C_{l,l}^{(1)} = c_{l,l}^{(1)}(z), \quad C_{l,g}^{(1)} = c_{l,g}^{(1)}(z), \quad C_{h,h}^{(1)} = c_{h,h}^{(1)}(\chi), \\ C_{h,l}^{(1)} = H_l^{(1)}(z) - C_{h,l}^{(0)} \otimes A_{ll}^{(1)}, \\ C_{h,g}^{(1)} = H_g^{(1)}(z) - C_{h,l}^{(0)} \otimes A_{lg}^{(1)} - C_{h,h}^{(0)} \otimes A_{hg}^{(1)}. \quad (4)$$

Here the lowercase coefficients  $c_{ij}^{(1)}(z)$  are given by their ZM expressions [28, 29].  $H_{l(g)}^{(1)}$  are the massive coefficients for CC at NLO [30–32], and  $A_{ij}$  are the corresponding operator-matrix elements (OMEs) [33]. Note that, in the FE contributions,  $z$  has been replaced by the scaling variable  $\chi$  according to the SACOT- $\chi$  convention.

There are several complications when extending to N<sup>2</sup>LO. Firstly, as mentioned, there are now HQ contributions to  $F_l$ ,

$$C_{l,g}^{(2)} = c_{l,g}^{(2)}(z), \quad C_{l,h}^{(2)} = c_{l,h}^{(2)}(\chi), \\ C_{l,l}^{(2)} = c_{l,l}^{(2)}(z) + \tilde{C}_{l,l}^{(NS,2)}(z), \quad (5)$$

where the N<sup>2</sup>LO ZM coefficient functions  $c_{i,j}^{(2)}(z)$  are calculated in Refs. [28, 29].  $\tilde{C}_{l,l}^{(NS,2)}$  denotes the non-singlet FC contribution after subtracting its massless counterpart, which has been included in  $c_{l,l}^{(2)}(z)$  to avoid double-counting. The expression for  $\tilde{C}_{l,l}^{(NS,2)}$ , with its full charm-quark mass dependence, can be found in Refs. [34–36]. For  $F_h$ , the N<sup>2</sup>LO FE and FC contributions are

$$C_{h,h}^{(2)} = c_{h,h}^{(2)}(\chi), \\ C_{h,l}^{(2)} = H_l^{(2)}(z) - \Delta C_{h,l}^{(2)}, \\ C_{h,g}^{(2)} = H_g^{(2)}(z) - \Delta C_{h,g}^{(2)}, \quad (6)$$

where the two-loop massive coefficient function  $H_{l(g)}^{(2)}$  is calculated numerically in Refs. [37, 38]. The subtraction terms,  $\Delta C_{h,l(g)}^{(2)}$ , can be constructed using the lower-order coefficient functions and the two-loop OMEs from Ref. [33]. Their full expressions are lengthy and will be included in a forthcoming paper.

Furthermore, the N<sup>3</sup>LO ZM coefficient functions for CC DIS have recently been calculated in Refs. [39–43] and implemented in the numerical program HOPPET [44, 45]. When  $Q^2 \gg M_Q^2$ , the ZM N<sup>3</sup>LO Wilson coefficients serve as the precise limit for the GM N<sup>3</sup>LO ones, while at  $Q^2 \approx M_Q^2$  they may miss potentially important mass-dependent contributions. In NC DIS, inclusion of analogous ZM N<sup>3</sup>LO contributions elevates the theoretical precision at large  $Q^2$  and lowers precision at the mass threshold compared to GM N<sup>2</sup>LO [46]. With these considerations, we also compute an *approximate* N<sup>3</sup>LO prediction, called GM N<sup>3</sup>LO', by adding the  $\mathcal{O}(\alpha_s^3)$  ZM contributions without  $\chi$  rescaling to the GM N<sup>2</sup>LO Wilson coefficients and using N<sup>2</sup>LO PDFs.

## PHENOMENOLOGY

We now summarize several phenomenological studies with our predictions incorporating full charm-quark mass effects. We use CT14 NNLO PDFs [47] with up to 3 active quark flavors for FFN predictions, and up to 4 active flavors with ZM and GM predictions. The charm-quark pole mass is taken to be 1.3 GeV, and the CKM matrix elements are chosen according to [1], in which the third generation is assumed to be diagonal. For the EW parameters, we use the  $G_F$  scheme [48]. We set the renormalization and factorization scales to the momentum transfer,  $\mu_R = \mu_F = Q$ , unless otherwise specified. After briefly considering our GM scheme for a generic reduced cross section, we highlight specific applications to neutrino-nucleus DIS and envisioned high- $Q^2$  measurements at the future EIC.

### A generic lepton-proton reduced cross section

Figure 2 compares predictions within the ZM and GM schemes for a reduced differential cross section  $d^2\sigma/(dx dQ^2)$  at a typical Bjorken- $x$  value of 0.02. The upper panel shows predictions for  $e^-p \rightarrow \nu_e X$  from NLO up to the highest available orders in the FFN and ZM schemes for  $2 \text{ GeV}^2 \leq Q^2 \leq 200 \text{ GeV}^2$ . At NLO, differences among the FFN and ZM predictions can reach 6% for high- $Q^2$  values. At N<sup>2</sup>LO,  $\lesssim 3\%$  differences persist at both the lowest and highest  $Q^2$ . The middle panel compares N<sup>2</sup>LO predictions for three schemes by showing ratios to the prediction of the GM scheme. Evidently, the GM prediction interpolates nicely between the ZM and

FFN predictions over a wide  $Q^2$  interval. The lower panel shows ratios of the GM predictions with scale variations at various  $\alpha_s$  orders. The scale variations are calculated by varying  $\mu_R$  and  $\mu_F$  simultaneously by a factor of two, while keeping them above the charm-quark mass. The N<sup>2</sup>LO prediction in the denominators assumes the nominal  $\mu_{R,F} = Q$  scales. The GM results converge well, and the scale dependence decreases prominently with the  $\alpha_s$  order. The scale dependence is truly small at high  $Q^2$  – about 1% for GM N<sup>2</sup>LO and just a few per mille for GM N<sup>3</sup>LO'. At  $Q^2 < 10 \text{ GeV}^2$ , the GM N<sup>2</sup>LO scale dependence of up to 5% remains substantial, in fact covering the differences between the three schemes at this order. The partial GM N<sup>3</sup>LO' prediction does not include the  $\mathcal{O}(\alpha_s^3)$  mass terms essential near the charm mass threshold, and in fact it needs not to converge at  $Q^2 \sim M_Q^2$ , yet it yields a smaller scale variation even at low  $Q$ .

In these calculations, we neglected contributions from bottom quarks, although their inclusion in our SACOT- $\chi$  formalism is straightforward. At high  $Q^2$ ,  $b$ -quark pairs can be produced in CC DIS via N<sup>2</sup>LO corrections, and there are virtual  $b$ -quark loops in gluon self-energy subgraphs. For a  $Q^2$  value of  $200 \text{ GeV}^2$ , and with the same setup as in Fig. 2, we found the bottom quark contributions to be small, about one per mille of the total cross section for a wide range of  $x$  values.

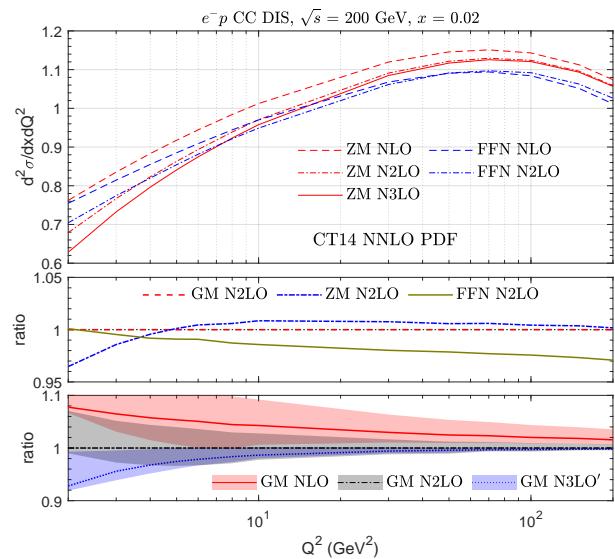


FIG. 2:  $Q^2$  dependence of differential reduced cross sections in  $e^-p$  CC DIS at  $\sqrt{s} = 200 \text{ GeV}$  for  $x = 0.02$ . Colored bands represent scale variations described in the main text.

### Neutrino DIS

Next, we turn to the inclusive CC DIS cross section for neutrino scattering off an isoscalar nuclear target as

a function of the neutrino energy,  $E_\nu$ . Figure 3 compares experimental measurements of neutrino-nucleus *total* inclusive cross sections divided by  $E_\nu$  to our predictions for CC DIS cross sections for  $E_\nu$  ranging from 5 to  $10^4$  GeV. We require  $Q^2 > 2 \text{ GeV}^2$  and  $W^2 > 4.9 \text{ GeV}^2$ . Many completed and upcoming fixed-target experiments have  $E_\nu < 400$  GeV. At very low  $E_\nu$ , the measured total cross section receives important quasi-elastic scattering and resonant production contributions [49] on the top of the DIS component that we compute. We stress that, even at a lower  $E_\nu$ , as in long-baseline experiments like DUNE [3], the CC DIS contribution remains important, accounting for more than 40% of the total event rate for  $E_\nu \sim 10$  GeV. As such, a few-percent correction to the DIS subprocess can be consequential to the ultimate precision of flavor-oscillation searches. DUNE, for instance, aims for percent-level precision in its neutrino oscillation search program. At high neutrino energies above 100 GeV the CC DIS is far dominant. The higher values of  $E_\nu$  considered here can be accessed at FASER $\nu$  [5] and IceCube [50].

In Fig. 3, the world-average value of  $\sigma_{CC}/E_\nu$  as reported in PDG20 [1], was originally documented in Ref. [51] by combining the CCFR90 [52], CCFRR [53], and CDHSW [54] measurements with  $E_\nu$  between 30 to 200 GeV. This is displayed as the black dashed line. The CCFR90 [52] measurements extract the total cross sections with an independent determination of the neutrino flux. On the other hand, CCFR96 [51], like many other neutrino-scattering experiments, only measured relative cross sections to cancel the neutrino flux uncertainty. The reported absolute cross sections as a function of  $E_\nu$ ,  $\sigma_{CC}/E_\nu$ , were obtained by matching onto the above-mentioned world-average value.

Our theory predictions include NLO EW corrections, as originally calculated in Ref. [55], and nucleon-level target mass corrections following the prescription of Ref. [56]. For  $E_\nu = 200$  GeV, these corrections increase the DIS cross section by about 2% and 1%, respectively. Furthermore, we check nuclear-to-isoscalar corrections using the nCTEQ15 PDFs [57], finding these only decrease cross sections by  $< 0.5\%$ , assuming  $A = 56$  for an iron nucleus. The upper panel of Fig. 3 shows the GM theory predictions at LO, NLO, N<sup>2</sup>LO and N<sup>3</sup>LO', as well as the ZM prediction at N<sup>3</sup>LO. QCD corrections reduce the LO cross sections by about 6% for most neutrino energies. The scale dependence indicated by the colored band is strongly reduced upon including higher-order corrections. The middle panel of Fig. 3 further compares theoretical predictions obtained at various QCD orders by examining ratios to the GM N<sup>2</sup>LO cross section. The scale variation for GM N<sup>2</sup>LO and especially N<sup>3</sup>LO' is negligible at  $E_\nu > 100$  GeV and is 1-3% otherwise. One important feature is that higher-order QCD corrections somewhat reduce the DIS cross section and increase the apparent difference between the precise CCFR96 data

and theory predictions, assuming the overall normalization of data determined as above. The agreement with the CCFR90 data is much better, especially for  $E_\nu$  above  $\approx 100$  GeV. The ambiguity due to the absent mass terms grows up to a few percent in the ZM and GM N<sup>3</sup>LO' predictions for the lowest  $E_\nu$ . This ambiguity is reduced in GM N<sup>2</sup>LO. These differences can be contrasted with the PDF uncertainties in the range 1~2% in the lower panel of Fig. 3. We also compared N<sup>2</sup>LO predictions using other PDF sets, MMHT2014 [58] and NNPDF3.1 [59]. They agree with CT14 within the PDF uncertainty.

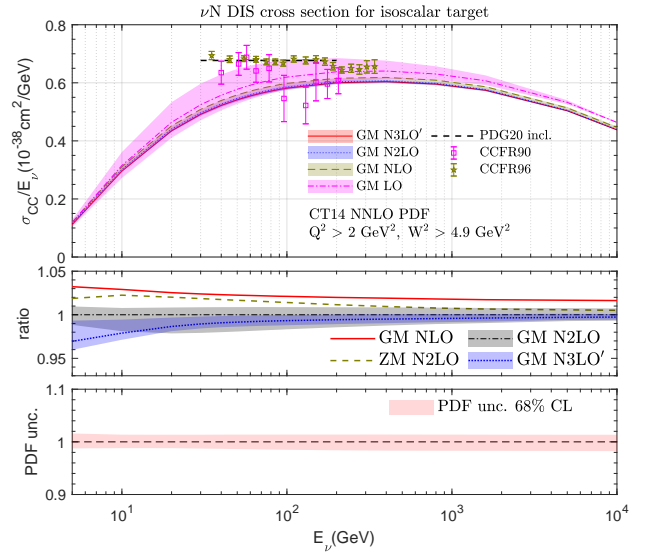


FIG. 3: Curved lines: the predicted CC DIS cross section in the SACOT- $\chi$  scheme at various orders versus the neutrino energy,  $E_\nu$ . Error bars and dashed horizontal line: CCFR measurements and the world average of the neutrino-nucleus total cross section. Colored bands in the upper/middle (lower) panel represent the scale variations (PDF uncertainty).

### HERA/EIC kinematics

Inclusive CC DIS can be measured precisely at a future EIC facility. At the lepton-hadron collider HERA and the EIC, typical  $Q^2$  in CC DIS are above  $100 \text{ GeV}^2$  due to difficulties of reconstruction of the full hadronic energy [8, 60]. Figure 4 shows reduced cross sections and ratios vs.  $x$  at  $Q^2 = 100 \text{ GeV}^2$  for  $e^-p$  collisions with a center-of-mass energy of 141 GeV. The comparison of GM predictions at various  $\alpha_s$  orders, including their scale variations, again demonstrates good perturbative convergence. At such  $Q^2$ , GM N<sup>3</sup>LO' is an excellent prediction, as the charm-mass terms are negligible. The GM N<sup>3</sup>LO' scale dependence is within 0.5-1%, except at very large  $x$ . By comparing the GM and ZM predictions, we find



that the full charm-quark mass effects can still lead to a correction of  $\approx 1\%$ , depending on the  $x$  values. The PDF uncertainties in the lower panel are generally about 2%. Such high theoretical accuracy is a step toward precision tests of QCD in CC DIS at the EIC.

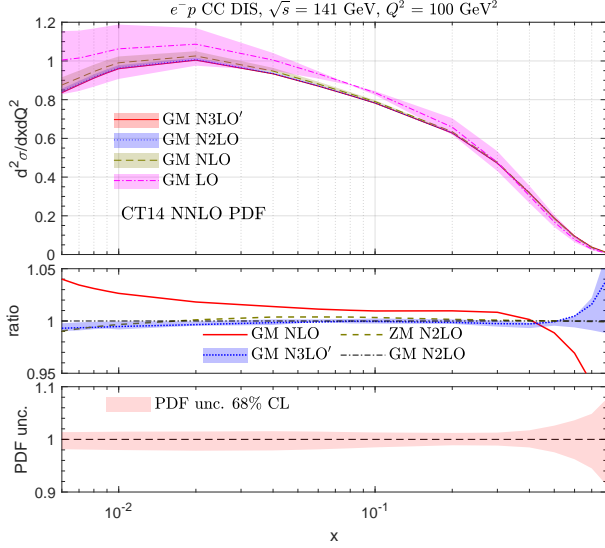


FIG. 4: Bjorken- $x$  dependence of differential reduced cross sections in  $e^-p$  CC DIS at  $\sqrt{s} = 141$  GeV for  $Q^2 = 100$  GeV $^2$ . Colored bands in the upper/middle (lower) panel represent the scale variations (PDF uncertainty).

In conclusion, we have presented a general-mass calculation for inclusive CC DIS at N $^2$ LO in QCD with full threshold dependence on the charm-quark mass. The GM N $^2$ LO predictions are consistent across a wide range of momentum transfers and have greatly reduced perturbative uncertainties. When appropriate, we augment the GM N $^2$ LO calculation by including the  $\mathcal{O}(\alpha_s^3)$  radiative contributions available in the zero-mass scheme. Our examination of phenomenological implications for several experimental programs, including neutrino experiments at various energies and the EIC, shows that perturbative uncertainties can be controlled at the level of a few percent and sometimes less.

This work is partially supported by the U.S. Department of Energy under Grant No. DE-SC0010129 (at SMU) and by the U.S. National Science Foundation under Grant No. PHY-2013791 at MSU. T. J. Hobbs acknowledges support from a JLab EIC Center Fellowship. The work of J.G. was supported by the National Natural Science Foundation of China under Grants No. 11875189 and No. 11835005. C.-P. Yuan is also grateful for the support from the Wu-Ki Tung endowed chair in particle physics.

- [1] P. A. Zyla et al. (Particle Data Group), PTEP **2020**, 083C01 (2020).
- [2] H. Abramowicz et al. (H1, ZEUS), Eur. Phys. J. C **75**, 580 (2015), 1506.06042.
- [3] R. Acciarri et al. (DUNE) (2015), 1512.06148.
- [4] J. Ahrens et al. (IceCube), Astropart. Phys. **20**, 507 (2004), astro-ph/0305196.
- [5] H. Abreu et al. (FASER) (2020), 2001.03073.
- [6] A. Accardi et al., Eur. Phys. J. A **52**, 268 (2016), 1212.1701.
- [7] R. Abdul Khalek et al. (2021), 2103.05419.
- [8] M. Arratia, Y. Furlotova, T. J. Hobbs, F. Olness, and S. J. Sekula, Phys. Rev. D **103**, 074023 (2021), 2006.12520.
- [9] E. Witten, Nucl. Phys. B **104**, 445 (1976).
- [10] R. M. Barnett, H. E. Haber, and D. E. Soper, Nucl. Phys. B **306**, 697 (1988).
- [11] F. I. Olness and W.-K. Tung, Nucl. Phys. B **308**, 813 (1988).
- [12] T.-J. Hou et al., Phys. Rev. D **103**, 014013 (2021), 1912.10053.
- [13] M. A. G. Aivazis, F. I. Olness, and W.-K. Tung, Phys. Rev. D **50**, 3085 (1994), hep-ph/9312318.
- [14] M. A. G. Aivazis, J. C. Collins, F. I. Olness, and W.-K. Tung, Phys. Rev. D **50**, 3102 (1994), hep-ph/9312319.
- [15] J. C. Collins, Phys. Rev. D **58**, 094002 (1998), hep-ph/9806259.
- [16] M. Krämer, F. I. Olness, and D. E. Soper, Phys. Rev. D **62**, 096007 (2000), hep-ph/0003035.
- [17] W.-K. Tung, S. Kretzer, and C. Schmidt, J. Phys. G **28**, 983 (2002), hep-ph/0110247.
- [18] R. S. Thorne and R. G. Roberts, Phys. Rev. D **57**, 6871 (1998), hep-ph/9709442.
- [19] S. Alekhin, J. Blumlein, S. Klein, and S. Moch, Phys. Rev. D **81**, 014032 (2010), 0908.2766.
- [20] S. Forte, E. Laenen, P. Nason, and J. Rojo, Nucl. Phys. B **834**, 116 (2010), 1001.2312.
- [21] M. Cacciari, M. Greco, and P. Nason, JHEP **05**, 007 (1998), hep-ph/9803400.
- [22] M. Cacciari, S. Frixione, N. Houdeau, M. L. Mangano, P. Nason, and G. Ridolfi, JHEP **10**, 137 (2012), 1205.6344.
- [23] B. A. Kniehl, G. Kramer, I. Schienbein, and H. Spiesberger, Phys. Rev. D **84**, 094026 (2011), 1109.2472.
- [24] B. A. Kniehl, G. Kramer, I. Schienbein, and H. Spiesberger, Eur. Phys. J. C **72**, 2082 (2012), 1202.0439.
- [25] I. Helenius and H. Paukkunen, JHEP **05**, 196 (2018), 1804.03557.
- [26] K. Xie, Ph.D. thesis, Southern Methodist U. (2019), chapter 10, URL [https://scholar.smu.edu/hum\\_sci\\_physics\\_etds/7/](https://scholar.smu.edu/hum_sci_physics_etds/7/).
- [27] M. Guzzi, P. M. Nadolsky, H.-L. Lai, and C. P. Yuan, Phys. Rev. D **86**, 053005 (2012), 1108.5112.
- [28] W. L. van Neerven and A. Vogt, Nucl. Phys. B **568**, 263 (2000), hep-ph/9907472.
- [29] W. L. van Neerven and A. Vogt, Nucl. Phys. B **588**, 345 (2000), hep-ph/0006154.
- [30] T. Gottschalk, Phys. Rev. D **23**, 56 (1981).
- [31] M. Gluck, S. Kretzer, and E. Reya, Phys. Lett. B **380**, 171 (1996), [Erratum: Phys.Lett.B 405, 391 (1997)], hep-ph/9603304.

- [32] J. Blümlein, A. Hasselhuhn, P. Kovacikova, and S. Moch, Phys. Lett. **B700**, 294 (2011), 1104.3449.
- [33] M. Buza, Y. Matiounine, J. Smith, and W. L. van Neerven, Eur. Phys. J. C **1**, 301 (1998), hep-ph/9612398.
- [34] M. Buza, Y. Matiounine, J. Smith, R. Migneron, and W. L. van Neerven, Nucl. Phys. B **472**, 611 (1996), hep-ph/9601302.
- [35] J. Blümlein, G. Falcioni, and A. De Freitas, Nucl. Phys. B **910**, 568 (2016), 1605.05541.
- [36] A. Behring, J. Blümlein, A. De Freitas, A. Hasselhuhn, A. von Manteuffel, and C. Schneider, Phys. Rev. **D92**, 114005 (2015), 1508.01449.
- [37] E. L. Berger, J. Gao, C. S. Li, Z. L. Liu, and H. X. Zhu, Phys. Rev. Lett. **116**, 212002 (2016), 1601.05430.
- [38] J. Gao, JHEP **02**, 026 (2018), 1710.04258.
- [39] S. Moch, J. A. M. Vermaseren, and A. Vogt, Phys. Lett. B **606**, 123 (2005), hep-ph/0411112.
- [40] J. A. M. Vermaseren, A. Vogt, and S. Moch, Nucl. Phys. B **724**, 3 (2005), hep-ph/0504242.
- [41] A. Vogt, S. Moch, and J. Vermaseren, Nucl. Phys. B Proc. Suppl. **160**, 44 (2006), hep-ph/0608307.
- [42] S. Moch, M. Rogal, and A. Vogt, Nucl. Phys. B **790**, 317 (2008), 0708.3731.
- [43] J. Davies, A. Vogt, S. Moch, and J. A. M. Vermaseren, PoS **DIS2016**, 059 (2016), 1606.08907.
- [44] G. P. Salam and J. Rojo, Comput. Phys. Commun. **180**, 120 (2009), 0804.3755.
- [45] F. A. Dreyer and A. Karlberg, Phys. Rev. D **98**, 114016 (2018), 1811.07906.
- [46] Bowen Wang, Ph.D. thesis, Southern Methodist U. (2015), chapter 4, URL <https://tinyurl.com/BowenWangThesis2015>.
- [47] S. Dulat, T.-J. Hou, J. Gao, M. Guzzi, J. Huston, P. Nadolsky, J. Pumplin, C. Schmidt, D. Stump, and C.-P. Yuan, Phys. Rev. D **93**, 033006 (2016), 1506.07443.
- [48] A. Denner and T. Sack, Nucl. Phys. B **358**, 46 (1991).
- [49] L. Alvarez-Ruso et al. (NuSTEC), Prog. Part. Nucl. Phys. **100**, 1 (2018), 1706.03621.
- [50] M. Bustamante and A. Connolly, Phys. Rev. Lett. **122**, 041101 (2019), 1711.11043.
- [51] W. G. Seligman, Ph.D. thesis, Nevis Labs, Columbia U. (1997).
- [52] P. S. Auchincloss et al., Z. Phys. C **48**, 411 (1990).
- [53] R. Blair et al., Phys. Rev. Lett. **51**, 343 (1983).
- [54] J. P. Berge et al., Z. Phys. C **35**, 443 (1987).
- [55] A. B. Arbuzov, D. Y. Bardin, and L. V. Kalinovskaya, JHEP **06**, 078 (2005), hep-ph/0407203.
- [56] H. Georgi and H. D. Politzer, Phys. Rev. D **14**, 1829 (1976).
- [57] K. Kovarik et al., Phys. Rev. D **93**, 085037 (2016), 1509.00792.
- [58] L. A. Harland-Lang, A. D. Martin, P. Motylinski, and R. S. Thorne, Eur. Phys. J. C **75**, 204 (2015), 1412.3989.
- [59] R. D. Ball et al. (NNPDF), Eur. Phys. J. C **77**, 663 (2017), 1706.00428.
- [60] E. C. Aschenauer, S. Fazio, J. H. Lee, H. Mantysaari, B. S. Page, B. Schenke, T. Ullrich, R. Venugopalan, and P. Zurita, Rept. Prog. Phys. **82**, 024301 (2019), 1708.01527.